

# 8.808/8.308 IAP 2026 Recitation 5: Entropy production by multiple temperatures

Jessica Metzger

jessmetz@mit.edu | Office hours: 1/9, 1/14, 1/20, 1/27 11am-12pm (8-320)

January 16, 2026

## Contents

1	Multi-temperature system	1
2	Entropy production	1
3	Non-equilibrium phenomenology	3
3.1	Run-and-chase motion	3
3.2	Ratchet currents	4
3.3	Many-body phenomenology: phase separation with no attraction	5
4	Numerics	6
4.1	Harmonic potentials	6
A	References	6

## 1 Multi-temperature system

Today, we study a system of two overdamped Brownian particles which are each connected to their own thermal reservoir, which may have *different* temperatures. This system is modeled by the Langevin dynamics

$$\dot{\mathbf{r}}_1(t) = -\nabla U(r_{12}) - \nabla V(\mathbf{r}_1) + \sqrt{2T_1}\boldsymbol{\eta}_1(t) \equiv \mathbf{f}_1(\mathbf{r}_1(t), \mathbf{r}_2(t)) + \sqrt{2T_1}\boldsymbol{\eta}_1(t) \quad (1)$$

$$\dot{\mathbf{r}}_2(t) = -\nabla U(r_{21}) - \nabla V(\mathbf{r}_2) + \sqrt{2T_2}\boldsymbol{\eta}_2(t) \equiv \mathbf{f}_2(\mathbf{r}_1(t), \mathbf{r}_2(t)) + \sqrt{2T_2}\boldsymbol{\eta}_2(t) . \quad (2)$$

where the noises  $\boldsymbol{\eta}_i$  are Gaussian white noises with statistics

$$\langle \eta_i^\alpha(t) \rangle = 0 , \quad \langle \eta_i^\alpha(t) \eta_j^\beta(t') \rangle = \delta^{\alpha\beta} \delta_{ij} \delta(t - t') . \quad (3)$$

Note that we are taking the mobilities to be unity  $\mu_1 = \mu_2 = 1$ , and are using units so the Boltzmann constant is also unity,  $k_B = 1$ .

Many processes in living systems can be understood as interactions between particles with different effective temperatures. For instance, in the genome, regions of high transcriptional activity receive fluctuations whose statistics are described by white noise of a higher temperature than transcriptionally inactive regions.<sup>1</sup> Moreover, attaching particles to different thermal reservoirs is a minimal way to break thermal equilibrium, and thus may help shed light on some universal properties of non-equilibrium systems. We will therefore try to understand this system from the standpoint of time-reversal symmetry violation, starting by proving that its entropy production rate is nonzero.

## 2 Entropy production

We will first compare the probabilities of trajectories and their reverses and calculate the entropy production rate. This system differs from the one studied in class, because there are noise sources with different strengths. Nevertheless, we still know the noise probabilities

$$P[\boldsymbol{\eta}_i(t)] \propto \exp\left(-\frac{1}{2} \int_0^{t_f} dt |\boldsymbol{\eta}_i(t)|^2\right) \quad (4)$$

---

<sup>1</sup>Goychuk et al. (2023), *Polymer folding through active processes recreates features of genome organization*, PNAS Vol. 120, No. 20.

and can thus convert to path probabilities using the relation

$$P[\mathbf{r}_1(t), \mathbf{r}_2(t)] = P[\boldsymbol{\eta}_1(t), \boldsymbol{\eta}_2(t)] \left| \frac{D[\boldsymbol{\eta}_1(t), \boldsymbol{\eta}_2(t)]}{D[\mathbf{r}_1(t), \mathbf{r}_2(t)]} \right| = P[\boldsymbol{\eta}_1(t)] P[\boldsymbol{\eta}_2(t)] \left| \frac{D[\boldsymbol{\eta}_1(t), \boldsymbol{\eta}_2(t)]}{D[\mathbf{r}_1(t), \mathbf{r}_2(t)]} \right|. \quad (5)$$

Before, for a single particle's trajectory  $x(t)$  with a force  $f(x(t))$ , we found that the Jacobian was of the form

$$\dot{x} = f(x(t)) + \eta \quad \Rightarrow \quad \left| \frac{D[\eta(t)]}{D[x(t)]} \right| \propto \exp \left( - \int_0^{t_f} \alpha f'(x(t)) dt \right). \quad (6)$$

For us, it is similar. We can show

$$\left| \frac{D[\boldsymbol{\eta}_1(t), \boldsymbol{\eta}_2(t)]}{D[\mathbf{r}_1(t), \mathbf{r}_2(t)]} \right| \propto \exp \left( - \int_0^{t_f} G(\mathbf{r}_1(t), \mathbf{r}_2(t)) \right) \quad (7)$$

for some function  $G$  which only depends on the locations of particles 1 and 2, not on their derivatives. We will not calculate this, because it will cancel with its time-reverse when we calculate entropy production. Thus, by substituting

$$\boldsymbol{\eta}_i(t) = \frac{\dot{\mathbf{r}}_i(t) - \mathbf{f}_i(t)}{\sqrt{2T_i}} \quad (8)$$

into Eq. (4), we find

$$P[\mathbf{r}_1(t), \mathbf{r}_2(t)] \propto \exp \left( - \int_0^{t_f} dt \left[ \frac{|\dot{\mathbf{r}}_1(t) - \mathbf{f}_1(t)|^2}{4T_1} + \frac{|\dot{\mathbf{r}}_2(t) - \mathbf{f}_2(t)|^2}{4T_2} + G(\mathbf{r}_1(t), \mathbf{r}_2(t)) \right] \right). \quad (9)$$

The probability of the trajectories' reverses,  $\mathbf{r}_1^R(t) = \mathbf{r}_1(t_f - t)$  and  $\mathbf{r}_2^R(t) = \mathbf{r}_2(t_f - t)$ , is then

$$P[\mathbf{r}_1^R, \mathbf{r}_2^R] \propto \exp \left( - \int_0^{t_f} dt \left[ \frac{|\dot{\mathbf{r}}_1^R(t) - \mathbf{f}_1^R(t)|^2}{4T_1} + \frac{|\dot{\mathbf{r}}_2^R(t) - \mathbf{f}_2^R(t)|^2}{4T_2} + G(\mathbf{r}_1^R(t), \mathbf{r}_2^R(t)) \right] \right) \quad (10)$$

$$= \exp \left( - \int_0^{t_f} dt \left[ \frac{|-\dot{\mathbf{r}}_1(t_f - t) - \mathbf{f}_1(t_f - t)|^2}{4T_1} + \frac{|-\dot{\mathbf{r}}_2(t_f - t) - \mathbf{f}_2(t_f - t)|^2}{4T_2} + G(\mathbf{r}_1(t_f - t), \mathbf{r}_2(t_f - t)) \right] \right) \quad (11)$$

$$= \exp \left( - \int_0^{t_f} dt \left[ \frac{|\dot{\mathbf{r}}_1(t) + \mathbf{f}_1(t)|^2}{4T_1} + \frac{|\dot{\mathbf{r}}_2(t) + \mathbf{f}_2(t)|^2}{4T_2} + G(\mathbf{r}_1(t), \mathbf{r}_2(t)) \right] \right). \quad (12)$$

The normalization constants for  $P[\mathbf{r}_1, \mathbf{r}_2]$  and  $P[\mathbf{r}_1^R, \mathbf{r}_2^R]$  are, again, identical. Thus, we can divide the path probabilities to find the entropy production

$$e^{\Sigma[\mathbf{r}_1, \mathbf{r}_2]} = \frac{P[\mathbf{r}_1, \mathbf{r}_2]}{P[\mathbf{r}_1^R, \mathbf{r}_2^R]} \quad (13)$$

$$= \exp \left( - \int_0^{t_f} dt \left[ \frac{|\dot{\mathbf{r}}_1(t) - \mathbf{f}_1(t)|^2}{4T_1} + \frac{|\dot{\mathbf{r}}_2(t) - \mathbf{f}_2(t)|^2}{4T_2} + G(\mathbf{r}_1(t), \mathbf{r}_2(t)) \right] \right) \quad (14)$$

$$+ \int_0^{t_f} dt \left[ \frac{|\dot{\mathbf{r}}_1(t) + \mathbf{f}_1(t)|^2}{4T_1} + \frac{|\dot{\mathbf{r}}_2(t) + \mathbf{f}_2(t)|^2}{4T_2} + G(\mathbf{r}_1(t), \mathbf{r}_2(t)) \right] \quad (15)$$

$$= \exp \left( \int_0^{t_f} dt \left[ \frac{\dot{\mathbf{r}}_1(t) \cdot \mathbf{f}_1(t)}{T_1} + \frac{\dot{\mathbf{r}}_2(t) \cdot \mathbf{f}_2(t)}{T_2} \right] \right) \quad (16)$$

and therefore

$$\Sigma[\mathbf{r}_1(t), \mathbf{r}_2(t)] = \int_0^{t_f} dt \left[ \frac{\dot{\mathbf{r}}_1(t) \cdot \mathbf{f}_1(t)}{T_1} + \frac{\dot{\mathbf{r}}_2(t) \cdot \mathbf{f}_2(t)}{T_2} \right] \quad (17)$$

$$= \int_0^{t_f} dt \left[ \frac{\dot{\mathbf{r}}_1(t)}{T_1} \cdot \left( -\nabla_1 U(r_{12}) - \nabla V(\mathbf{r}_1) \right) + \frac{\dot{\mathbf{r}}_2(t)}{T_2} \cdot \left( -\nabla_2 U(r_{12}) - \nabla V(\mathbf{r}_2) \right) \right] \quad (18)$$

$$= - \int_0^{t_f} dt \frac{\dot{\mathbf{r}}_1(t) \cdot \nabla V(\mathbf{r}_1(t))}{T_1} - \int_0^{t_f} dt \frac{\dot{\mathbf{r}}_2(t) \cdot \nabla V(\mathbf{r}_2(t))}{T_2} - \int_0^{t_f} dt \nabla_1 U(r_{12}) \cdot \left[ \frac{\dot{\mathbf{r}}_1}{T_1} - \frac{\dot{\mathbf{r}}_2}{T_2} \right] \quad (19)$$

$$= - \frac{[V(\mathbf{r}_1(t_f)) - V(\mathbf{r}_1(0))]}{T_1} - \frac{[V(\mathbf{r}_2(t_f)) - V(\mathbf{r}_2(0))]}{T_2} - \int_0^{t_f} dt \nabla_1 U(r_{12}) \cdot \left[ \frac{\dot{\mathbf{r}}_1}{T_1} - \frac{\dot{\mathbf{r}}_2}{T_2} \right]. \quad (20)$$

We have used the chain rule to simplify

$$\frac{d}{dt} V(\mathbf{r}_i(t)) = \dot{\mathbf{r}}_i(t) \cdot \nabla V(\mathbf{r}_i(t)) . \quad (21)$$

This is fine, because we have been implicitly using Stratonovich calculus from the beginning. (If we had been using Itô calculus, the conversion between forward and reverse trajectory probabilities wouldn't have been as simple, and the integrals would be interpreted differently.) Finally, the entropy production *rate*,  $\sigma$ , is given by the time-average of the entropy production,  $\Sigma$ . The terms involving the potential energy differences go away for a bounded  $V$  in the  $t_f \rightarrow \infty$  limit. However, the final term can't be written as a total derivative: we have

$$\frac{d}{dt} U(r_{12}) = \dot{\mathbf{r}}_1 \cdot \nabla_1 U(r_{12}) + \dot{\mathbf{r}}_2 \cdot \nabla_2 U(r_{12}) = \dot{\mathbf{r}}_1 \cdot \nabla_1 U(r_{12}) - \dot{\mathbf{r}}_2 \cdot \nabla_1 U(r_{12}) = [\dot{\mathbf{r}}_1 - \dot{\mathbf{r}}_2] \cdot \nabla_1 U(r_{12}) \quad (22)$$

This is proportional to  $(\frac{\dot{\mathbf{r}}_1}{T_1} - \frac{\dot{\mathbf{r}}_2}{T_2}) \cdot \nabla_1 U(r_{12})$  if and only if the temperatures are equal. Thus if the temperatures are unequal, this term grows linearly in time, while the  $\Delta V(\mathbf{r}_i)$  terms plateau.

The entropy production rate is thus given by

$$\sigma = \lim_{t_f \rightarrow \infty} \frac{1}{t_f} \Sigma[\mathbf{r}_1(t), \mathbf{r}_2(t)] = \lim_{t_f \rightarrow \infty} \frac{1}{t_f} \int_0^{t_f} dt \nabla U(\mathbf{r}_1 - \mathbf{r}_2) \cdot \left[ \frac{\dot{\mathbf{r}}_1}{T_1} - \frac{\dot{\mathbf{r}}_2}{T_2} \right] , \quad (23)$$

which is nonzero if and only if  $T_1 \neq T_2$ .

Note that, after some manipulation, we can see that  $\sigma$  is simply the Kullback-Leibler divergence of the probability distribution of forward and reverse trajectories:

$$\sigma = \lim_{t_f \rightarrow \infty} \frac{1}{t_f} \ln \left( \frac{P[\mathbf{r}_1, \mathbf{r}_2]}{P[\mathbf{r}_1^R, \mathbf{r}_2^R]} \right) \stackrel{\text{ergodicity}}{=} \left\langle \ln \left( \frac{P[\mathbf{r}_1, \mathbf{r}_2]}{P[\mathbf{r}_1^R, \mathbf{r}_2^R]} \right) \right\rangle = \int D[\mathbf{r}_1, \mathbf{r}_2] P[\mathbf{r}_1, \mathbf{r}_2] \ln \left( \frac{P[\mathbf{r}_1, \mathbf{r}_2]}{P[\mathbf{r}_1^R, \mathbf{r}_2^R]} \right) \quad (24)$$

$$= D_{\text{KL}}(P \parallel P^R) , \quad \text{where} \quad P^R[\mathbf{r}_1, \mathbf{r}_2] \equiv P[\mathbf{r}_1^R, \mathbf{r}_2^R] . \quad (25)$$

The Kullback-Leibler divergence is a measure of statistical indistinguishability between two distributions. The fact that  $\sigma \neq 0$  means that if we are played a movie of the steady-state dynamics and told that there's a 50% chance it's being played in reverse, we can do better than 50/50 in guessing which direction it's being played in.

Finally, note that the units of  $\sigma$  are  $T^{-1}$  (inverse time). The inverse of  $\sigma$  gives a timescale, which is approximately the amount of time you need to watch the dynamics before being relatively certain of the direction they're being played. Thus if  $\sigma$  is huge, you almost immediately know if it's running backwards, while if  $\sigma$  is small, you need to collect more data.

### 3 Non-equilibrium phenomenology

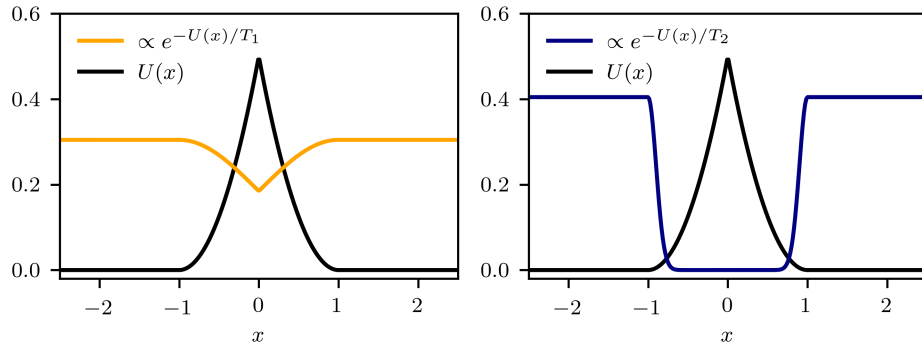
We have proven that the entropy production rate is nonzero, and therefore that the system violates time-reversal symmetry. This has a number of interesting consequences.

#### 3.1 Run-and-chase motion

Consider a pair of hot and cold particles interacting through the purely repulsive potential

$$U(r) = \begin{cases} \frac{k}{2} \left(1 - \frac{r}{\sigma}\right)^2 , & r < 1 \\ 0 , & \text{otherwise} \end{cases} , \quad (26)$$

where  $\sigma$  is some length scale determining the maximum interaction distance. The dynamics display an effective nonreciprocity, because cold particles are much more sensitive to the effects of potentials than hot particles are. To see this, imagine a *fixed* potential  $U(x)$ , and a single particle  $x_1$  of temperature  $T_1$  experiencing it. It will take on the Boltzmann distribution  $P(x_1) \propto e^{-U(x_1)/T_1}$ . If  $T_1$  is high,  $P(x_1)$  will be relatively flat. However, for a different particle  $x_2$  of lower temperature  $T_2 \ll T_1$ ,  $P(x_2) \propto e^{-U(x_2)/T_2}$  will be much more sensitive to  $U$ . This is visualized below:

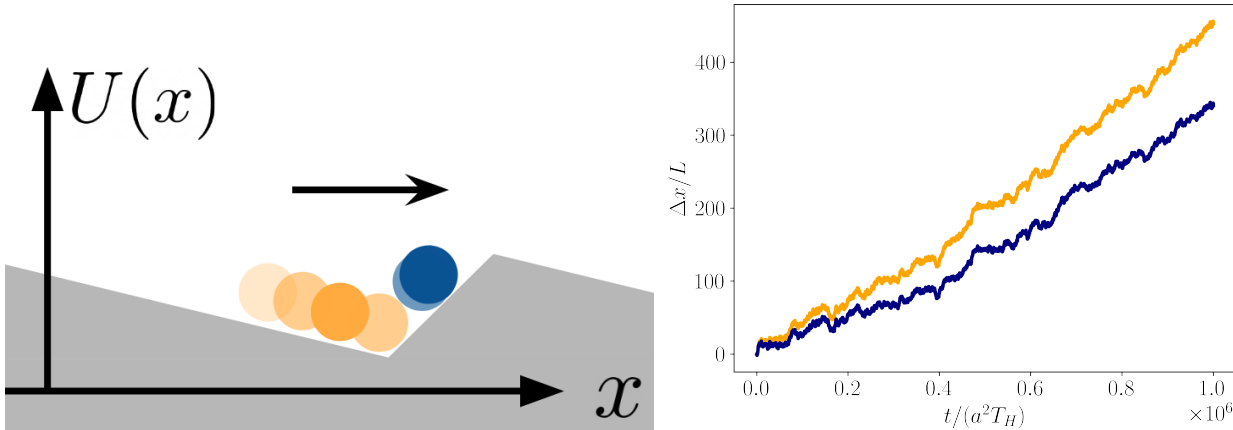


Now consider the fact that, in each point in time, particle 1 experiences particle 2 as a potential (albeit a moving one), and particle 2 experiences particle 1 as the same potential. Thermal fluctuations cause the hotter particle to move closer to the colder particle within the interaction length, which isn't too unlikely because the hotter particle is relatively insensitive to the cold particle's potential. But when this happens, the cold particle moves down the potential it experiences from the hot particle. Thus creates an effective run-and-chase dynamics, where motion of the particles' center of mass is biased towards the direction of  $\mathbf{r}_2 - \mathbf{r}_1$ :

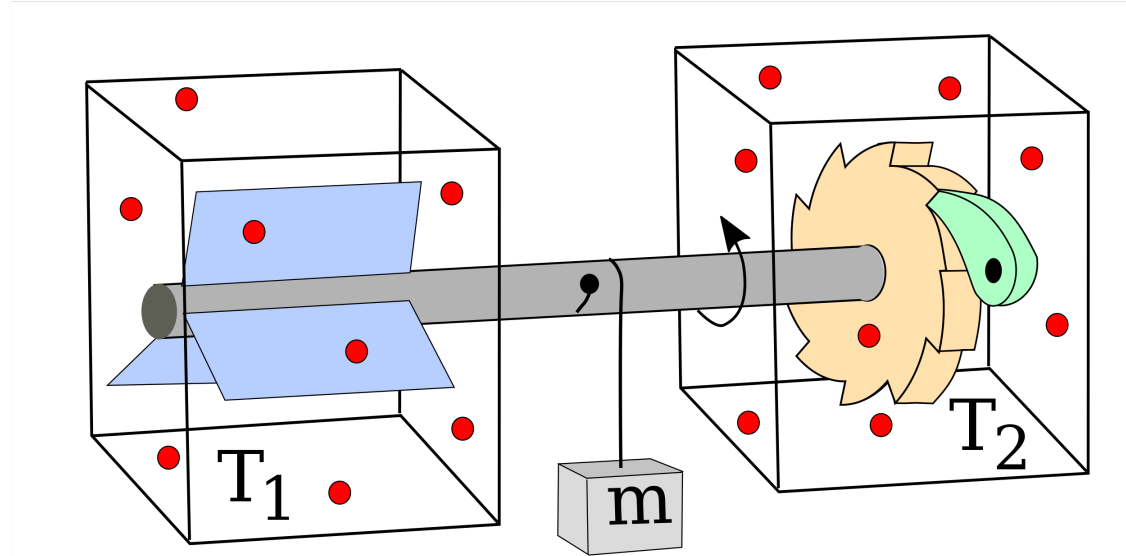


### 3.2 Ratchet currents

When placed in an asymmetric external potential  $V(x)$ , e.g. a sawtooth potential, 2-temperature pairs exhibit steady-state currents (“ratchet currents”). This is, in fact, expected, because the environment breaks parity symmetry, and the difference in temperatures breaks time-reversal symmetry. The microscopic origin of the ratchet current for repulsive 2-temperature pairs can be understood as a consequence of the run-and-chase dynamics discussed above: the hot particle pushes the cold particle (an inherently non-equilibrium phenomenon), and it is easier to push it over one side of the potential than the other:

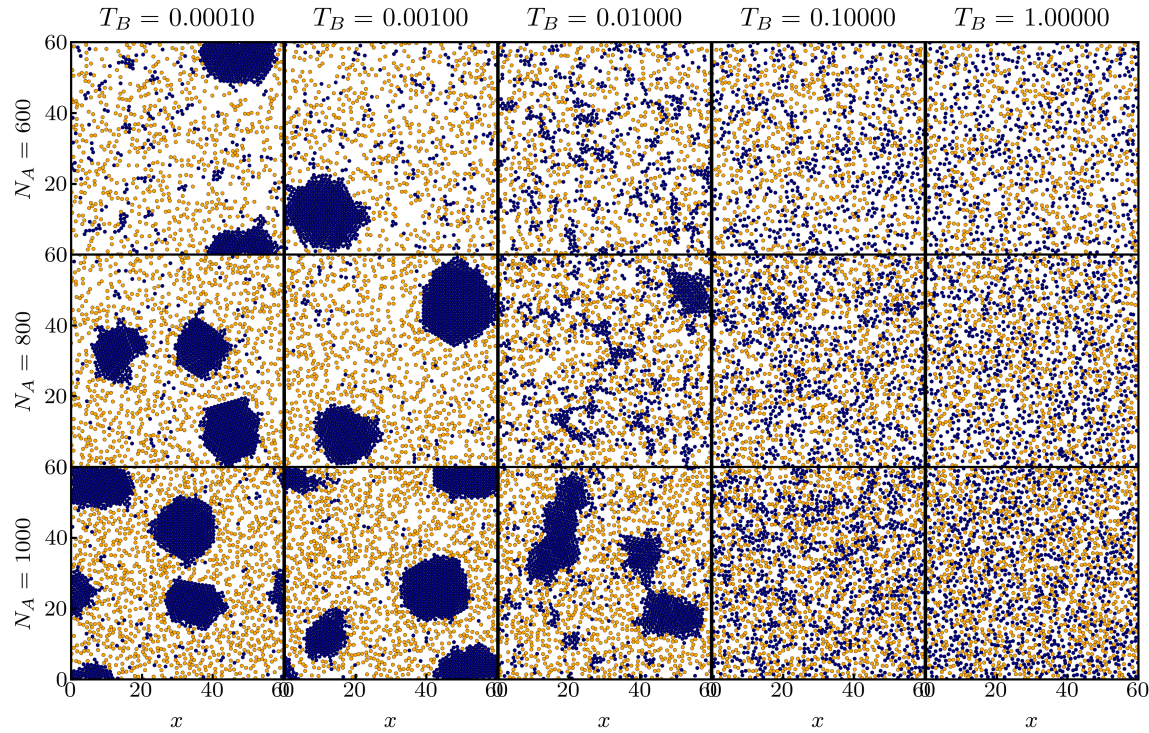


Also, the Feynman ratchet, impossible in an isothermal setting, can be realized through a temperature difference:



### 3.3 Many-body phenomenology: phase separation with no attraction

When you place many purely repulsive hot and cold particles together, if the temperature difference is high enough and the repulsion is strong enough, they will phase separate into a dilute gas of hot particles and a dense liquid or solid of cold particles. In equilibrium, phase separation is driven by attractive forces overcoming the loss in mixing entropy. For identically-sized hot and cold particles, packing cold particles in a dense cluster both increases energy and loses entropy. Thus, this phase separation is driven by purely non-equilibrium effects. I show some simulation snapshots below (if left to evolve, the cold droplets in phase-separating systems will coarsen into a single, roughly circular droplet):

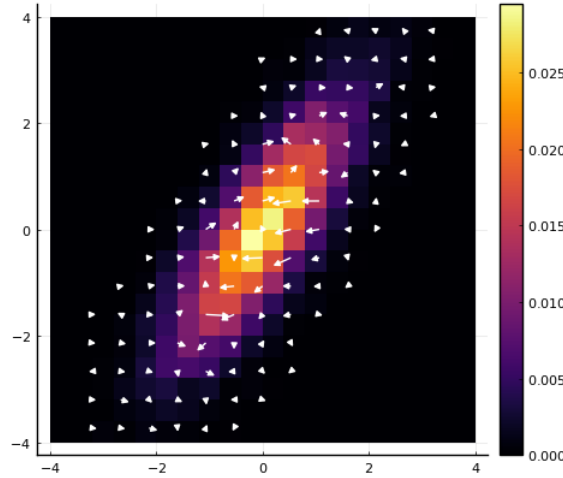


This hot-cold phase segregation has been invoked as a mechanism for organization of transcriptionally active and inactive genetic material in the nucleus.

## 4 Numerics

We will simulate the 2-temperature 2-particle system with harmonic interactions, in a harmonic potential, in  $d = 1$  spatial dimension. We will generate density heatmaps in the  $(x_1, x_2)$  joint phase space, along with the current field. The code can be found on the website: [Rec5\\_2temp.jl](#) and [Rec5\\_module.jl](#)

The result looks something like this:



The  $x$ -axis,  $x_1$ , is the position of particle 1 (hot). The  $y$ -axis,  $x_2$ , is the position of particle 2 (cold). The existence of steady-state fluxes in this phase space signifies violation of time-reversal symmetry.

### 4.1 Harmonic potentials

In the case where  $U$  and  $V$  are both harmonic:

$$U(r) \equiv \frac{k}{2}r^2, \quad V(\mathbf{r}) \equiv \frac{\lambda}{2}|\mathbf{r}|^2, \quad (27)$$

the Langevin dynamics (1)-(2) become

$$\dot{\mathbf{r}}_1 = -k(\mathbf{r}_1 - \mathbf{r}_2) - \lambda\mathbf{r}_2 + \sqrt{2T_1}\boldsymbol{\eta}_1 \quad (28)$$

$$\dot{\mathbf{r}}_2 = -k(\mathbf{r}_2 - \mathbf{r}_1) - \lambda\mathbf{r}_1 + \sqrt{2T_2}\boldsymbol{\eta}_2. \quad (29)$$

## A References

- 2-temperatures with harmonic potentials: Dotsenko et al. (2013), *Two temperature Langevin dynamics in a parabolic potential*, Phys. Rev. E 87, 062130
- Entropy production of 2 temperatures with harmonic potentials (including model-free measurement of the entropy production rate): Li et al. (2019), *Quantifying dissipation using fluctuating currents*, Nat. Comm. 10:1666. (among others)
- Many-body 2-temperature system:
  - Awazu (2014), *Segregation and phase inversion of strongly and weakly fluctuating Brownian particle mixtures and a chain of such particle mixtures in spherical containers*, Phys. Rev. E 90, 042308
  - Grosberg and Joanny (2015), *Nonequilibrium statistical mechanics of mixtures of particles in contact with different thermostats*, Phys. Rev. E 92, 032118.
  - Weber et al. (2016), *Binary Mixtures of Particles with Different Diffusivities Demix*, Phys. Rev. L 116, 058301.
  - Goychuk et al. (2023), *Polymer folding through active processes recreates features of genome organization*, PNAS Vol. 120, No. 20.